Combination of focused ion beam (FIB) and transmission electron microscopy (TEM) as sub-0.25 mm defect characterization tool

Yih-Yuh Doong*, Jui-Mei Fu, Yong-Fen Hsieh

Now with *Worldwide Semiconductor Manufacturing Crop.

*E-mail: kelvin_doong@usa.net

United Microelectronics Corp.

ABSTRACT

A sub-0.25 μm defect characterization study was conducted by using in-line inspection machines to locate defects and focused ion beam system (FIB) equipped with a navigation tool[1-3] to generate cross-sectional transmission electron microscopy (TEM) samples[4-8]. Two failure analysis cases regarding to invisible defects in optical microscope were reported in this work. One described the micro-trench formed at the bird's beak of field oxide, and the other one illustrated the etching pit formation during Poly-Si etching process.

INTRODUCTION

As the advent of device scaling and process complication, failure analysis and material characterization have been pushed to their limits and beyond. Within most of failure analysis tools, transmission electron microscopy (TEM) is being seen as the most promising one providing extremely high spatial resolution image of integrated circuit for sub-micron process analysis. Unfortunately, conventional TEM specimen preparation is labor-intensive, lower success rate of specific site specimen preparation and is difficult to address the position of a cross-section specimen with sub-micron precision. Therefore, it is an obstacle to enact this technique to analyze the defect reviewed by automatic inspection equipment such as KLA, Tencor, Inspex, Orbot, and etc. In practice, this problem is circumvented by marking the site of interest with a laser. Owing to the resolution of optical microscopy and artifact induced by laser marker, this scheme can not exactly locate the defect classified by the automatic inspection equipment, and is throughput-limited. Whereas the application of TEM in the defect reduction of wafer level is thus far rather restrained.

The introduction of focused ion beam system (FIB) has been proven to be a significant step in analyzing defects and identifying at which process the defects are introduced. Because of the computer-controlled stage, navigation software and its in-situ high resolution (~ 10 nm) imaging capability, FIB system can drive the wafer to the defect location with the accuracy of um range and mill micron even to sub-micron scale features at the a specific site. By combining the capability of the high spatial resolution imaging of TEM, the high accuracy positioning and sub-micron milling of FIB system, the material characterization of the sub-0.25 μm defect reviewed by inspection apparatus can be greatly increased the efficiency and precision without artifacts. In this paper, two cases of application of this revolutionary scheme in analysis of in-line process defects detected by KLA 2135 will be presented.

ANALYSIS FLOW

Defect inspection machine, KLA 2135, was used. The defect detection methods were categorized into two techniques: die-to-die and cell-to-cell comparisons, the former provides defect detection in all types of circuit patterns, and the latter utilizes areas of a device, which have geometry that repeats. By setting the sensitivity and corresponding speed for the throughput, both patterned and unpatterned wafers could be inspected. The defect data file including die location, coordinates, size, and type were saved in the database and transferred to the FIB system equipped with a navigation tool prior to future analysis. Figure 1 shows that the defect wafer map was transferred from the defect data file loaded from the network.

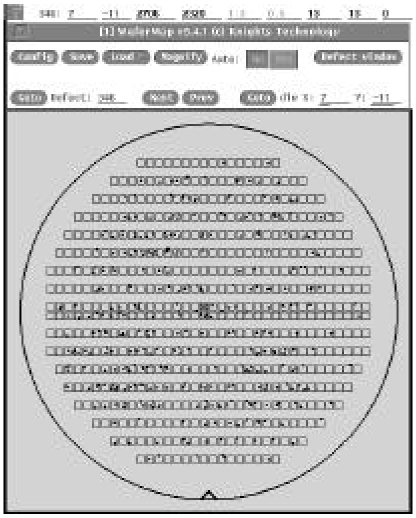

Figure 1: Defect wafer map was transferred from the in-line inspection equipment. With the aid of navigation tool, wafer was driven to the defect site directly in FIB chamber.

FIB fabrication was carried out with dual beam system from FEI Inc. model DualBeam 820 which combines the field-emission SEM for navigation and high resolution imaging; the focused ion beam for milling and deposition. FIB process includes two major steps: marking and TEM sample preparation. Through the integrated navigation control interface, the wafer can be automatically driven to the defect location on the inspection tool wafer maps. Square-shaped marking was performed around the defect as a indicator of OM observation and Pt was deposited on the surface to prevent damage during the mechanical lapping (Figure 2).

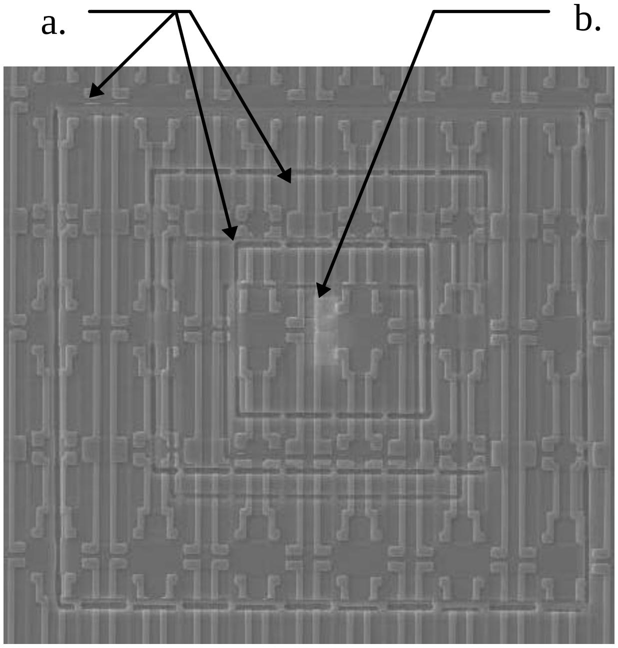

Figure 2: SEM micrograph of defect after FIB specific marking.

After marking and Pt deposition done at the sites of interest, the wafer is loaded out FIB chamber and cleaved, lapped down to 20 ~ 50 μm thick, and mounted to a modified copper grid prior to FIB process for TEM sample preparation. The mechanical polishing is similar to the techniques developed by Morris, S. et al. except the shape and position of modified copper grid which prevents the gas nozzle hitting the TEM sample (Figure 3, 4). Before FIB fabrication, the TEM sample was coated with metal film of several hundred Å thick as a conductive path preventing charging.

The FIB fabrication procedure used for this work is illustrated in Figure 5. Two trenches were milled on the both sides of the TEM sample by FIB with Halogen gas assisted[9-10]. Two kinds of Halogen gas are available for this work: XeF_2 and I_2. Due to the high etching rate of XeF_2, XeF_2 is not suitable for longer time etching. FIB milling using I_2 gas with larger current mode (870 pA) was performed until the thickness of the TEM sample reached 1μm. After initial trenches milled, the successive steps with progressively reducing the ion beam current (300 pA, 150 pA, and 60 pA, respectively) were enacted to mill the TEM membrane down to 100 ~ 150 nm thick. To remove the skirt of the tapered TEM membrane, the incident angle of the ion beam was set $3^o \sim 5^o$ off from the vertical to the specimen surface. Figure 6 shows the TEM membrane process flow fabricated by FIB.

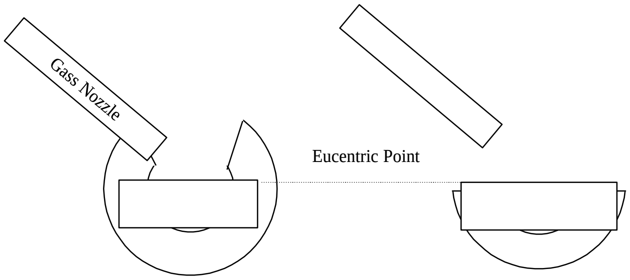

Figure 3: The left is used by Morris, S. et al. and the right is used in this work. The right can prevent the gas nozzle hitting the sample but the left.

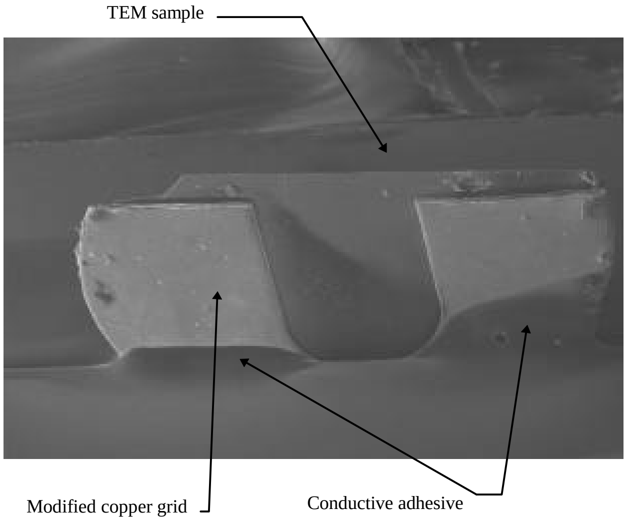

Figure 4. SEM micrograph of TEM sample mounted on the modified copper grid.

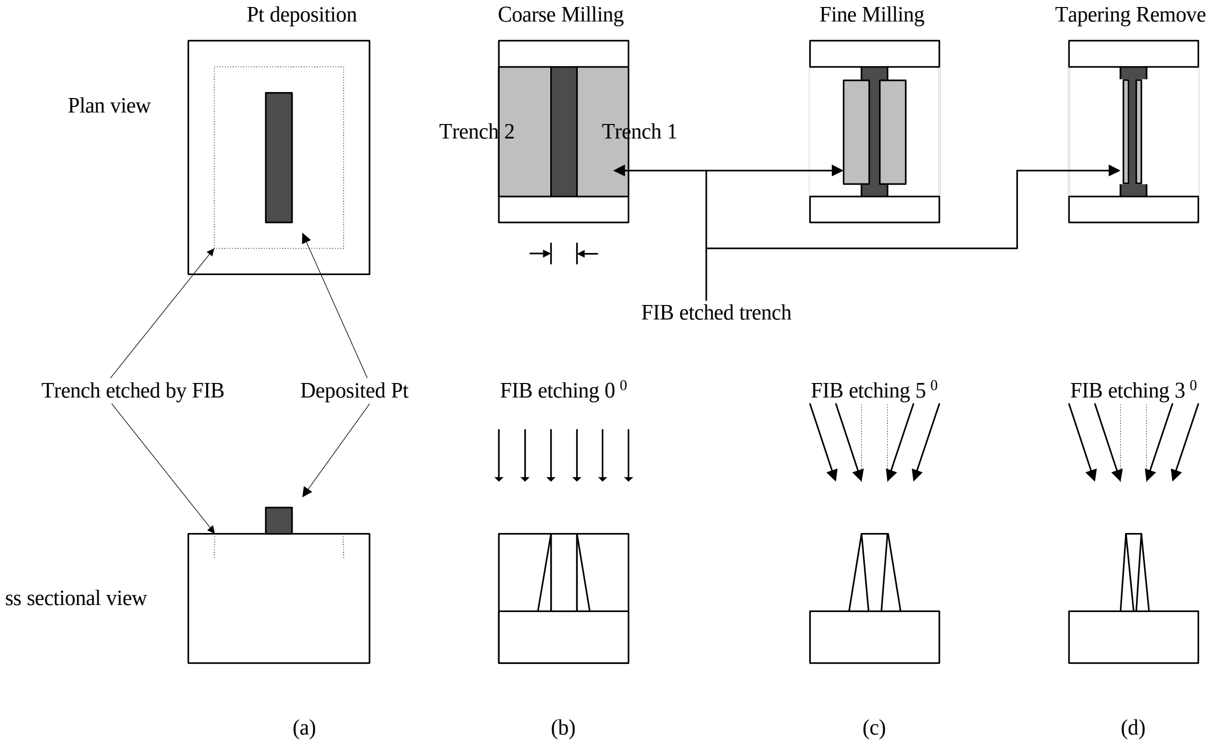

Figure 5: FIB fabrication procedure. (a) Pt deposition and marking. (b) Coarse milling: Ion beam vertical milling trench with I_2 gas until thickness reaches 1 λm. (c) Fine milling: Ion beam set 5^0 off from vertical without I_2 gas. (d) Tapering remove: Ion beam set 3^0 off from vertical without I_2 gas.

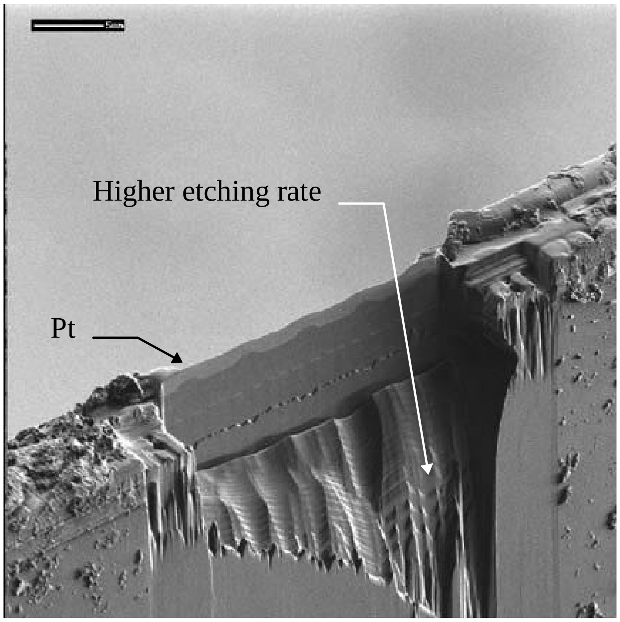

Figure 6: The TEM membrane fabricated by FIB. Due to the I_2 gas flux from the LH side, the etching rate of the RH side trench is higher than the LH side.

The TEM micrograph presented in the work had been made with JEOL TEM 2010 with the accelerating voltage of 200 KeV.

The complete sub-0.25 µm defect analysis flow was showed in Figure 7. Defect monitoring inspections were included in the IC fabrication process. If the number of defects was out of spec, wafers were pulled for more detailed characterization by in-line FE-SEM/ EDS. Whence the in-line analysis tools did not reveal detailed information, wafers were sent to the off-line material analysis laboratory. Most of defects which of size were bigger than 1µm were characterized and analyzed by cross-sectioning process. Few of defects, which size was smaller than 1 µm were subjected to cross-sectional TEM observation. With Dualbeam 820’s 8-inch wafer capability, extremely accurate stage navigation, the analysis would be routinely done under one working day.

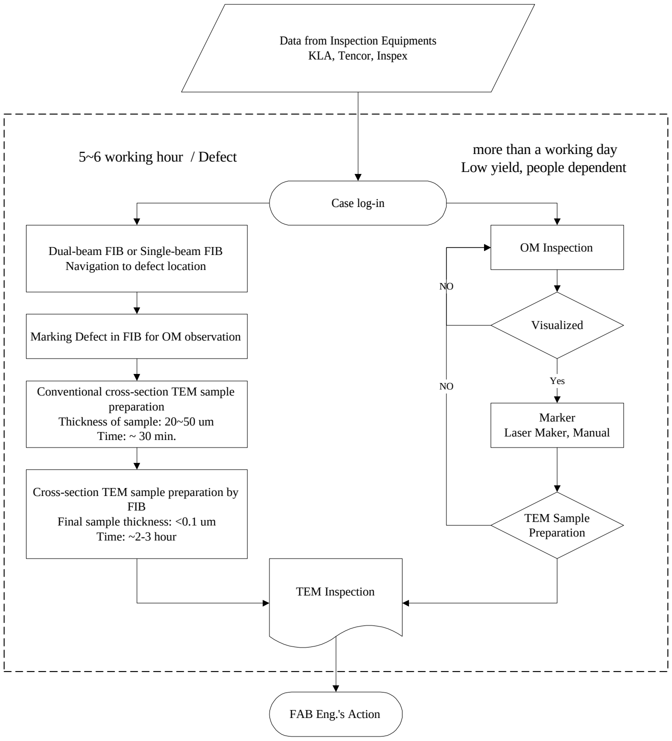

Figure 7: A sub-0.25 um defect characterization process flow. The processes inside the dashed line were carried out at the off-line materials analysis laboratory.

Examples

Defect monitoring inspections including several process steps such as lithography, deposition, and etch were regularly run through at the fab to check proper equipment condition and process variation. After ADI /AEI, a defect wafer map file and its corresponding SEM micrograph were sent to the material analyst prior to further analysis. The following examples use this novel technology to investigate several defect types.

Micro-trench at bird's beak

Defect was observed after Poly1 patterning inspection by KLA. Cross-sectional SEM sample was prepared perpendicularly through the micro trench (Figure 8, 9). However, SEM resolution is not high enough to reveal the defect structure. XTEM analysis was chosen because of the TEM superior spatial resolution capabilities.

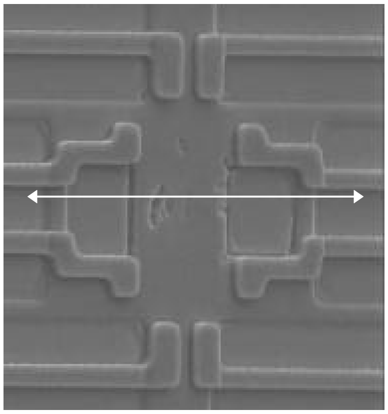

Figure 8: SEM micrograph of defect. XSEM sample was prepared along the white line.

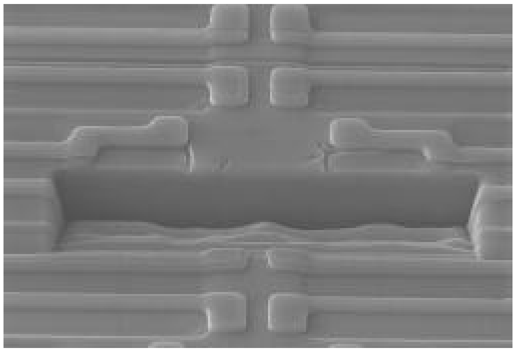

Figure 9: XSEM micrograph of defect in Figure 8. SEM micrograph can not reveal the fine structure of defect.

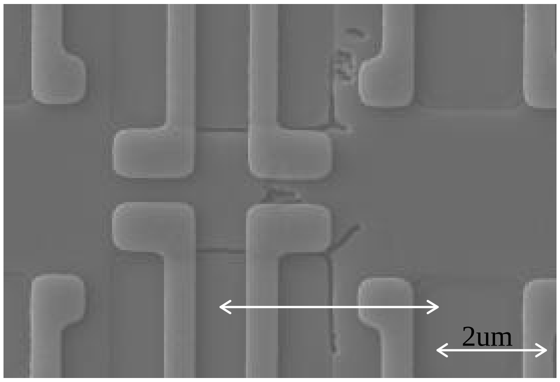

Figure 10: SEM micrograph of Defect. Cross-sectional TEM (XTEM) sample was taken along the white line.

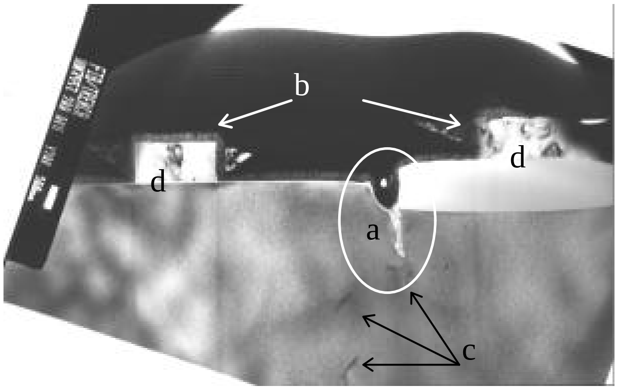

Figure 11: XTEM micrograph of Defect in Figure 10. Enlarged micrograph of circle area shown in Figure 12.

(a) micro-trench at the bird's beak,
(b) TiN film deposited to prevent charging effect during SEM and FIB observation,
(c) Dislocation, (d)Poly gate, (e) sacrificial Pt film.

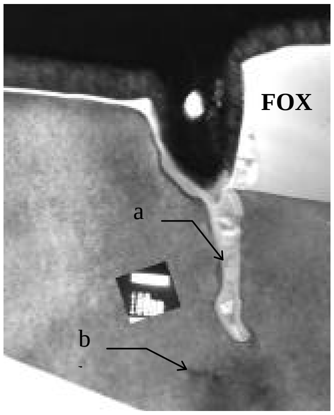

Fig. 12: XTEM micrograph of defect.
(a) Poly-Si, (b) dislocation.

Etching pits

Defect suspected as etching pits were detected after Poly1 patterning inspection. Due to the obstacle of OM observation during TEM sample preparation, this novel technique was performed as analysis method.

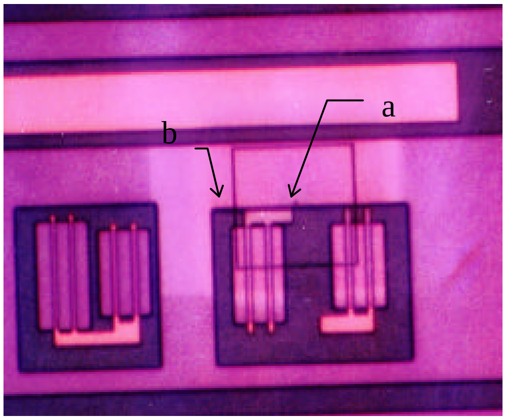

Figure 13: Optical micrograph of etching pit. (a) etching pit, (b) square mark etched by FIB.

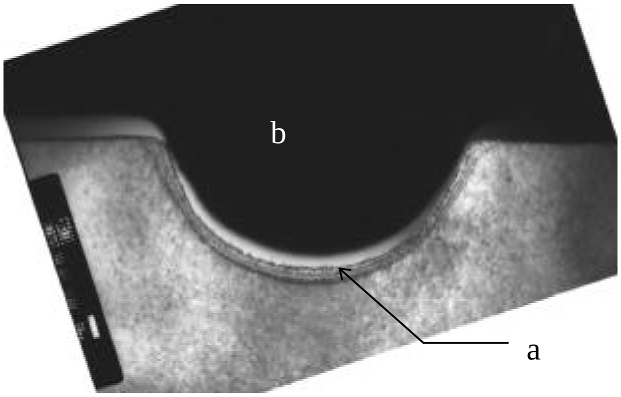

Figure 14: XTEM micrograph of etching pit. (a) Oxide. (b) Sacrificial Pt film

Summary

This technique provides a timely, reliable, and high yield method to analyze sub-0.25 µm defect. Combining the CAD navigation tool, specific site TEM sample preparation can be routinely done and more analyst-independent. The total analysis can be done under working day.

References:

1. L. Liu, N. Doan, P. Wang, Proc. ISTFA`95, p.231-234 (1995).
2. P. Catinella and B. Edwards, ISTFA`93, p.397-404 (1993).
3. A.B. Soto and S.L. Riley, ISTFA`93, p.419-424 (1993).
4. S. Morris, S. Tatti, E. Black, N. Dickson, H. Mendez, B. Schwiesow, and R. Pyle, ISTFA`91, p.417-427 (1991).
5. John F. Walker, FEI Europe Ltd.'s internal document.
6. John F. Walker, FEI Europe Ltd.'s internal document.
7. M.H. Overwijk, F.C. van den Heuvel, and C.W. T. Bulle-lieuwma, JVST B11(6), p.2021-2024 (1993).
8. C.W. Snyder, M.R. Frei, D. Bahnck, L. Hopkins, R. Hull, L. Harriott, T.Y. Chiu, T. Fullowan, and B. Tseng, JVST B13(4), p1514-1518 (1995)
9. Akira Yamaguchi and Takeshi Nishikawa, JVST B13(3), p.962-966 (1995).
10. Akira Yamaguchi and Masahiro Shibata, JVST B11(6), p.2016-2020 (1993).